CrossMark

ORIGINAL ARTICLE

Effects of Paclitaxel and Eribulin in Mouse Sciatic Nerve: A Microtubule-Based Rationale for the Differential Induction of Chemotherapy-Induced Peripheral Neuropathy

Sarah J. Benbow[1,2] · Brett M. Cook[1,3] · Jack Reifert[1,2] · Krystyna M. Wozniak[4] ·
Barbara S. Slusher[4,5] · Bruce A. Littlefield[6] · Leslie Wilson[1,2] · Mary Ann Jordan[1,2] ·
Stuart C. Feinstein[1,2]

Abstract Microtubule targeting agents (MTAs) often lead to treatment limiting and life threatening side effects, including chemotherapy-induced peripheral neuropathy (CIPN). The frequency of severe CIPN varies among different MTAs. Since the microtubule binding interactions and mechanisms of action also vary among MTAs, we hypothesized that these distinct mechanisms may underlie the variability in frequency of severe CIPN. Using a two-week, maximum tolerated dose model, we morphologically and biochemically analyzed sciatic nerves from mice treated with either paclitaxel or eribulin. These drugs differ in their manner of microtubule binding and mechanisms of action and reports indicate paclitaxel also induces a higher frequency of severe CIPN than does eribulin. Morphologically, paclitaxel increased the frequency of observed signs of axon degeneration more significantly than did eribulin. Alternatively, eribulin but not paclitaxel induced occasional myelin "halo" structures. Biochemically, paclitaxel, and eribulin both induced α-tubulin expression (∼1.9- and ∼2.5-fold, respectively) and tubulin acetylation, a marker for microtubule stability, (∼5- and ∼11.7-fold, respectively). Eribulin but not paclitaxel-induced EB1 expression ∼2.2-fold while paclitaxel but not eribulin mildly suppressed EB3 expression. Both EB proteins are associated with microtubule growth. Eribulin's combination of relatively mild deleterious morphological effects coupled with more potent biochemical changes promoting microtubule stability and growth in mice correlate with lower frequencies of severe CIPN in humans. We suggest that these eribulin-induced effects create a relatively stable microtubule network that compensates, in part, for the toxic anti-cancer effects of the drug, leading to fewer reported incidences of CIPN than for paclitaxel.

Electronic supplementary material The online version of this article (doi:10.1007/s12640-015-9580-6) contains supplementary material, which is available to authorized users.

✉ Stuart C. Feinstein
feinstei@lifesci.ucsb.edu

1 Neuroscience Research Institute, University of California, Santa Barbara, CA 93106, USA

2 Department of Molecular, Cellular and Developmental Biology, University of California, Santa Barbara, CA, USA

3 Program in Biomolecular Sciences and Engineering, University of California, Santa Barbara, CA, USA

4 Johns Hopkins Drug Discovery Program, Johns Hopkins School of Medicine, Baltimore, MD, USA

5 Departments of Neurology, Psychiatry and Neuroscience, Johns Hopkins School of Medicine, Baltimore, MD, USA

6 Eisai Inc., Andover, MA, USA

Introduction

The anti-tumor activity of MTAs stems from their ability to alter normal regulatory mechanisms controlling microtubule dynamics and microtubule-based transport, which can in turn lead to tumor cell death (Argyriou et al. 2012; Field et al. 2014; Jordan and Wilson 2004; Poruchynsky et al. 2015). Unfortunately, MTAs also expose non-target tissues to chemical assault that can cause significant adverse side effects. As the peripheral nervous system is highly susceptible to deleterious MTA-induced effects, chemotherapy-induced peripheral neuropathy (CIPN) is among the most frequent and serious side effects of MTA

treatment. CIPN can cause symptoms ranging from numbness and tingling to hypersensitivity and severe neuropathic pain. These symptoms generally begin at the distal extremities, such as the fingertips and toes, and progress proximally toward the trunk, suggesting that the longest axons are the most vulnerable (Argyriou et al. 2012; Carlson and Ocean 2011; Windebank and Grisold 2008). These symptoms can become treatment limiting, and in some cases, even life threatening. The only strategies to address CIPN are to either reduce drug dosage or cease treatment altogether, both of which undermine attempts to control a patient's cancer. Since MTAs are a major component of available clinical anti-cancer strategies, CIPN can be a major obstacle to successful clinical anti-cancer efforts.

The severity, clinical presentation and reversibility of neuropathic symptoms can vary greatly between different MTA treatments (Argyriou et al. 2011, 2012; Carlson and Ocean 2011; Windebank and Grisold 2008). For example, paclitaxel-treated patients generally exhibit a higher frequency of severe neuropathy than do eribulin-treated patients (Carlson and Ocean 2011; Gradishar 2011). Consistent with these observations, paclitaxel treatment of mice causes significant axon loss, morphological changes in myelin and reduction of nerve conduction velocity whereas eribulin treatment generated significantly milder morphological changes with no impairment of conduction velocity (Boehmerle et al. 2014; Wozniak et al. 2011). Importantly, different MTAs also differ greatly in their mechanisms of microtubule binding and their effects upon microtubule dynamics. For example, the taxanes (e.g., paclitaxel) bind the inner surface along the entire length of microtubules, tend to stabilize microtubules and to promote net microtubule polymerization. These activities are driven, in large part, by suppression of microtubule shortening events (Derry et al. 1995). In contrast, eribulin (a halichondrin) binds only at the plus (+) ends of microtubules, promotes microtubule dynamic instability and promotes net microtubule depolymerization. These activities are driven, in large part, by binding to soluble tubulin and shifting the balance between soluble tubulin and microtubules, thus resulting in net loss of microtubule polymer (Jordan et al. 2005; Smith et al. 2010). Over the past two decades, it has become increasingly clear that the regulation of microtubule growing and shortening events is key to understanding microtubule action and the resulting cellular consequences, thereby providing a potential molecular link between MTA action and clinical observations. Taken together, these observations lead us to hypothesize that different patterns of CIPN induced by different MTAs are the result of their different underlying mechanisms of action.

In addition to their important roles in dividing cells (i.e., cell division and transport), microtubules are also essential for many functions in post-mitotic mature neurons, including the maintenance of highly elongated neuronal morphologies and axonal transport, the rapid movement of cargo between neuronal cell bodies and distal axonal regions (Carlson and Ocean 2011). One often stated hypothesis for MTA-induced CIPN posits that the drugs interfere with normal microtubule-dependent axonal transport, which in turn initiates downstream biochemical and morphological neurodegeneration (Morfini et al. 2009). Consistent with this model, paclitaxel treatment can slow the rate of kinesin-driven anterograde transport more than eribulin treatment (Lapointe et al. 2013), in parallel with the relative neuropathic potencies of these two drugs.

Cells possess numerous mechanisms to regulate microtubule dynamics. For example, α-tubulin subunits in relatively stable microtubules are often acetylated at lysine-40. While tubulin acetylation has historically been viewed as a marker but not a cause of microtubule stability, recent work suggests a more active role. For example, increasing α-tubulin acetylation can rescue dysfunctional axonal transport and locomotor deficits in Drosophila (Godena et al. 2014) and can promote recruitment of dynein and kinesin-1 to microtubules in vitro and in mammalian cells (Dompierre et al. 2007). Additionally, microtubule dynamics can be influenced by a number of different microtubule-associated proteins (MAPs), including the end binding proteins EB1 and EB3. EB1 has been implicated in promoting microtubule growth and axonal transport while EB3 can serve as a link between dynamic microtubules and the actin cytoskeleton (Geraldo et al. 2008; Gu et al. 2006; Jaworski et al. 2009). We have previously proposed that proper function and viability of cells, including post-mitotic neurons, requires that cells actively maintain, and regulate their microtubule dynamics within a window of tolerable activity levels (Bunker et al. 2004)—both overly dynamic and overly stable microtubules can lead to neuronal cell death.

Here, we sought to compare cellular and molecular changes within mouse sciatic nerves following treatment with two different MTAs possessing different mechanisms of action and different probabilities of inducing severe CIPN. The goal was to correlate cellular and molecular effects with the frequency of inducing severe CIPN. Specifically, we compared mice treated at their maximum tolerated dose (MTD) of either paclitaxel or eribulin with vehicle-treated control mice. We found that paclitaxel induced markedly more deleterious effects upon sciatic nerve morphology, such as nerve fiber loss and signs of axon degeneration (for example, solid circular regions of myelin signal lacking a phosphoneurofilament signal), relative to the effects of eribulin. Additionally, eribulin had more potent positive effects upon microtubule biochemistry, creating an environment consistent with increased

microtubule stabilization and growth. Taken together, we propose that response to eribulin treatment generates a more stable and functional microtubule network than that produced by paclitaxel treatment. This perspective provides a molecular rationale for the observation that eribulin induces less frequent CIPN than does paclitaxel in human patients.

Materials and Methods

Antibodies

The following primary antibodies were used in immuno-histochemical analyses: anti-α-tubulin [Millipore, 04-1117, 1:100 dilution (Zhang et al. 2011)], anti-acetylated tubulin [Cell Signal, 5335, 1:800 dilution, (Creppe et al. 2009)], anti-EB1 [Millipore, AB6057, 1:500 dilution, (Vitre et al. 2008)], anti-EB3 [Santa Cruz, SC-101475, 1:200 dilution, (Levy et al. 1994)], anti-myelin basic protein [Millipore, AB9348, 1:100 dilution, (Heller et al. 2014), anti-phosphoneurofilament (Covance, SMI-31R, 1:2000 dilution, (Choi et al. 2008)]. FITC, Cy3, and Cy5 conjugated secondary antibodies were purchased from Jackson ImmunoResearch and used at 1:200 dilution.

Drugs

Eribulin mesylate (synthesized at Eisai Research Institute and stored at −80 °C in the dark) was dissolved in 100 % anhydrous DMSO (Sigma-Aldrich) to produce a 10 mg/ml stock solution, which was aliquoted and stored at −80 °C until the day of administration. Each administration day, the stock solution was thawed and diluted with saline to a final concentration of 0.25 mg/mL in 2.5 % DMSO/97.5 % saline yielding dosing solutions in a 10 mL/kg volume. Paclitaxel, (LC Laboratories, Woburn, MA; stored at −20 °C in the dark) was dissolved in ethanol (100 %) at 10 % of final volume. An equal volume of cremophor (10 % of final volume) was then added and the mixture re-vortexed for about 10 min. Immediately prior to injection, ice cold saline was added to final volume (as 80 % of final), and the solution was maintained on ice during dosing. Dosing solutions were made fresh daily and dosed in a volume of 10 mL/kg.

Animal Studies

Female BALB/c mice (approximately 7–8 weeks old at onset of dosing) were obtained from Harlan Laboratories Inc. (Indianapolis, IN) and maintained with free access to water and a standardized synthetic diet (Harlan Teklab). Animal housing and procedure room temperature and humidity were maintained at $20 \pm 2^{\circ}$ C and 55 ± 10 %, respectively. Artificial lighting provided a 12 h light/12 h dark cycle (light 7 a.m.–7 p.m.). All experimental protocols were approved by the Institutional Animal Care and Use Committee of Sobran Inc (Baltimore, MD, USA) and adhered to all of the applicable institutional and governmental guidelines for the humane treatment of laboratory animals.

Mice were randomly assigned into vehicle, eribulin or paclitaxel treatment group ($n = 5$).

Drugs were administered three times a week (Monday, Wednesday, Friday) for 2 weeks into the caudal vein at a dose that was earlier determined to be MTD (Wozniak et al. 2011), specifically 30 and 1.25 mg/kg for paclitaxel and eribulin, respectively. Twenty-four hours after administration of the sixth and final dose, mice were deeply anesthetized with 10 % chloral hydrate and euthanized by transcardial perfusion with PBS followed by 4 % paraformaldehyde in 0.1 mM phosphate buffer, pH 7.4, for 10–15 min. Subsequently whole mid-thigh sections of sciatic nerve were dissected and placed in perfusion fixative at 4 °C.

Sectioning

Fixed nerves were embedded in 10 % agarose and cross-sectioned using a Leica VT1000S vibratome. 100 μm slices were taken in the distal to proximal direction in 1X PBS at room temperature, then transferred to a 4 % paraformaldehyde/PBS solution for storage at 4° C until staining. Approximately 0.75 cm of Sciatic nerve tissue was sectioned.

Antibody Staining

Sections were stained from both proximal and distal ends from a total approximate length of 0.75 cm of nerve. Individual sections were stained with antibodies recognizing α-tubulin, acetylated tubulin, EB1, or EB3. All sections were also stained with anti-phosphoneurofilament and anti-myelin basic protein as internal controls and in order to identify regions of interest (for example, neuronal cells). Sections were incubated in PBT blocking agent (1X PBS (1.37 M NaCl, 27 mM KCl, 100 mM Na_2HPO_4, 18 mM KH_2PO_4), 0.1 % TritonX-100, 1 % BSA, 1 % donkey serum) overnight. Sections were then incubated free-floating with primary antibodies for seven days, rocking at 4 °C. The long duration of incubation was used to promote better antibody penetration. Primary antibody dilution solutions were removed and sections washed four times with PBT on a shaker at room temperature (8 min/wash). Sections were next incubated with secondary antibodies for 2 days. Secondary antibody dilutions were removed and sections washed as described above. Sections were then

mounted on glass slides using ProLong Gold mounting media with DAPI (Life Technologies P36935). Slides were sealed and stored at 4 °C. Each slide contained one section from each of the four treatments (eribulin and its vehicle, paclitaxel and its vehicle, Figure S1A), all stained simultaneously with the same antibody solution.

Fluorescence Microscopy

Images were collected using an Olympus Fluoview 1000 Spectral confocal system equipped with 405, 488, 559, and 635 nm laser lines, and PMT detectors. Each slide containing one section from each of the four treatments and incubated in the same antibody solution was imaged with the same exposure settings, determined by identifying the brightest-fluorescing section on each slide. 20 μm sample depths of two sections from each nerve (one relatively proximal and one relatively distal) were imaged by sequential laser scanning and 0.5 μm step size with an Olympus PLANAPOSC 60x (1.40 NA) high refractive index oil immersion objective. In practice, we imaged and assessed at least 160 μm of tissue from the 0.75 cm nerve length. This corresponds to 20 μm sections for each α-tubulin, acetylated tubulin, EB1 and EB3, or 80 μm total from each end. Two additional sections were cut from each end for backup and/or testing of other antibodies. As noted above, all sections were also stained with anti-MBP and anti-phosphoneurofilament. Where applicable, the anti-MBP and anti-phosphoneurofilament signals in these additional sections were included in the statistical analyses.

Image and Statistical Analysis

Images from each slide were imported into Imaris Version 7.5.2 (Bitplane, Zurich, Switzerland) and rendered into three dimensional maximum intensity z-stack projections for analysis.

To assess changes in gross morphological structure, nuclei, myelin, and axons were identified using DAPI stain, anti-myelin basic protein, and anti-phosphoneurofilament, respectively. Using the Imaris software surfaces tool, we identified nuclei, myelin sheaths, and axons based on the fluorescent signal from their appropriate antibody or stain, manually thresholding signal to background noise. To maintain consistency in object identification in similarly treated samples, one set of threshold parameters was applied to those sections stained with the same antibody solutions and imaged with the same microscope settings. After identification, these objects were counted automatically. Signs of axon degeneration, defined as solid, circular regions of myelin lacking a phosphoneurofilament signal, were identified and counted manually and compared with the total number of myelin objects identified by the

software. For axon density measurements, the image stack was flattened in Fiji using the maximum intensity setting and the number of axons per region of interest (defined by phosphoneurofilament signal) was quantified using Imaris.

In order to quantify fluorescence changes, fluorescence values were collected and normalized within each slide first, before comparisons were made between slides. Normalization of axonal Cy2 fluorescent signals (depicted in Supplementary Figure S1) was accomplished by using the anti-phosphoneurofilament (PNF) signal to identify and mask the axonal regions, specifically differentiating axons from surrounding Schwann cells or other cell types present. The raw values of Cy2 fluorescence were determined for each axonal region within the treatment field of view. The mean Cy2 signal per axon was calculated for each treatment to give the "treatment mean." These values were normalized by dividing each treatment mean by the sum of all four treatment means per slide. This method was employed in order to retain the natural variability seen in vehicle treatments.

Student's t tests with Bonferroni correction for multiple comparisons were used to identify significant differences in mean comparisons of the drug groups to their respective vehicles and between the two drug treatment groups, ($*p < 0.0167$, $**p < 0.003$, $***p < 0.0003$). In some cases, the singular comparison of the drug to appropriate vehicle group by Student's t test provided additional insight.

Results

Paclitaxel and Eribulin Differentially Induce Morphological Changes

We began our analyses by quantifying the neurodegenerative effects of paclitaxel and eribulin on sciatic nerve axon density, defined by anti-phosphoneurofilament (PNF) signal, in cross-sections of nerves from drug-treated mice and vehicle-treated controls. Paclitaxel treatment resulted in a statistically significant 30 % reduction in axon density (196.3 ± 18.52 axons per 10^4 μm^2 compared to 281.8 ± 22.2 axons per 10^4 μm^2 for its vehicle control; Figs. 1a, b, 2a, b). In contrast, eribulin administration generated a 21 % reduction in axon density (234.1 ± 18.52 axons per 10^4 μm^2 compared to 296.6 ± 18.43 per 10^4 μm^2 for its vehicle controls (mean $\pm$ SEM; Figs. 1a, b, 2c, d). While neither of these reductions are statistically significant when compared using a Bonferroni corrected Student's t test, it appears that the densities reported here trend toward axonal loss after treatment with both eribulin and paclitaxel.

We next sought to examine the effects of paclitaxel and eribulin upon axon-myelin morphology by quantifying the
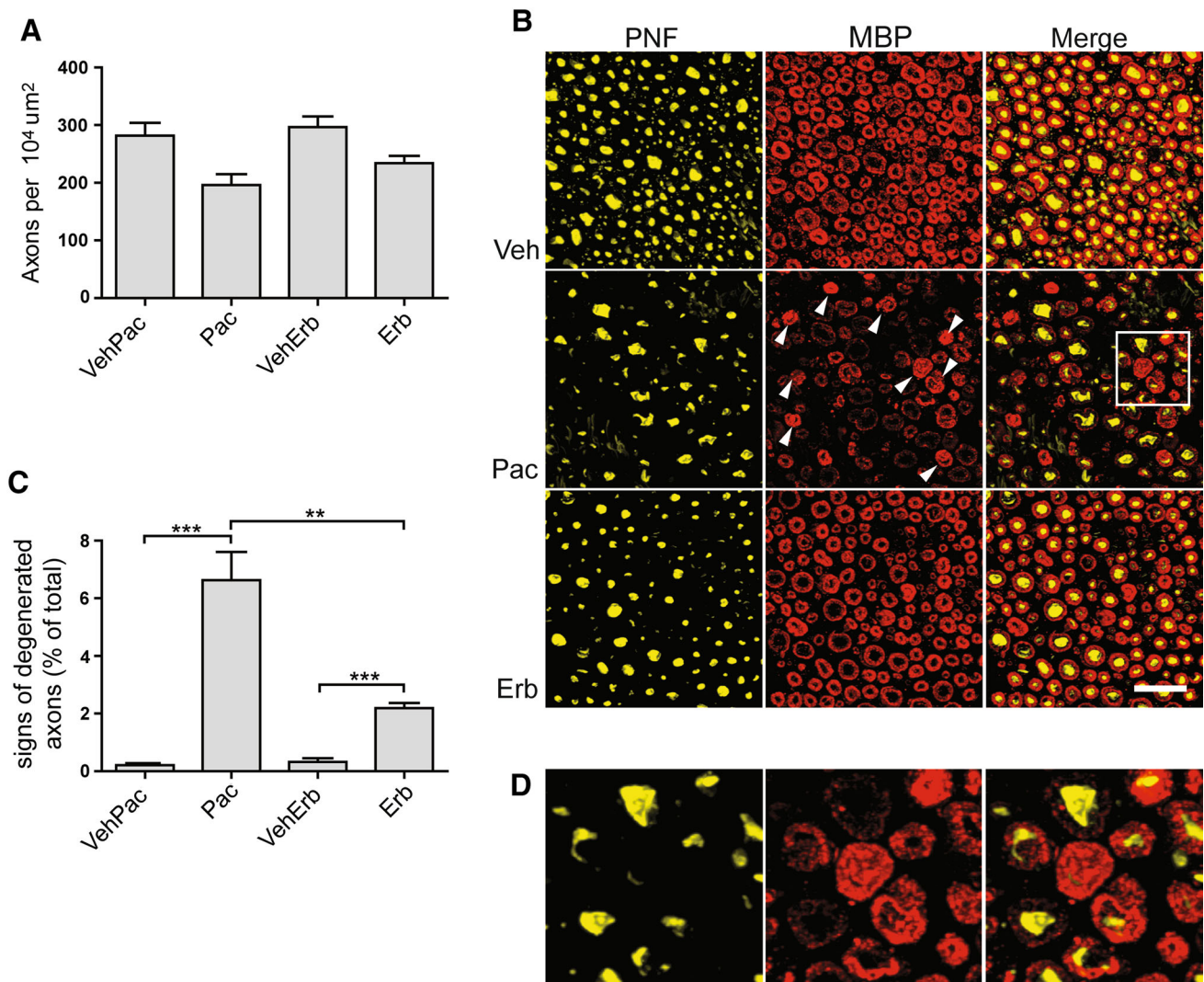
Fig. 1 Paclitaxel and eribulin differentially affect sciatic nerve morphology. **a** Quantification of axon density per 10^4 μm^2. ($n = 5$, $p > 0.0167$) **b** Representative confocal images of paclitaxel and eribulin-treated sciatic nerves; phosphoneurofilament (*yellow*), myelin basic protein (*red*). *White arrow heads* indicate observed signs of axon degeneration. **c** Quantification of observable signs of axon degeneration per total number of anti-myelin basic protein (MBP) stained objects, **$p < 0.003$, ***$p < 0.0003$. **d** Enlarged region of paclitaxel image to show axon degenerative events from boxed area indicated on panel C. *Scale bar* 20 μm

extent of fiber disruption in cross-sections of sciatic nerves harvested from drug-treated mice relative to vehicle-treated, control animals. Paclitaxel treatment increased the percent of observed signs of axon degeneration relative to total myelin positive objects. "Signs of axon degeneration" are defined as structures with clear anti-myelin basic protein (MBP) signals but lacking any anti-PNF signal (Figs. 1b–d, 2). Specifically, we observed 6.6 % of myelin sheaths (anti-MBP stained objects) in paclitaxel-treated nerves exhibiting signs of axon degeneration (vs. 0.21 % for vehicle-treated nerves; $p < 0.0003$). In contrast, eribulin induced three-fold fewer degenerative axons (2.2 vs. 0.32 % for vehicle-treated nerves; $p < 0.0003$). Additionally the difference between

paclitaxel and eribulin-treated groups is also statistically significant ($p < 0.003$). Similar degenerative events have been described in several instances of neuronal toxicity and injury, where the space normally occupied by the axon is lost and has been replaced by myelin (Muguruma et al. 2006; Schnaar et al. 2014; Wozniak et al. 2011). Additionally, in nerves from both paclitaxel and eribulin-treated mice, we qualitatively observed an increase in myelin fragmentation (thinning and discontinuity of sheath) that often lacked an associated phosphoneurofilament stain (For example, see Fig. 2e–h). Given that these morphological changes were almost exclusively observed in tissue from drug-treated mice, we conclude that these are treatment-induced changes.
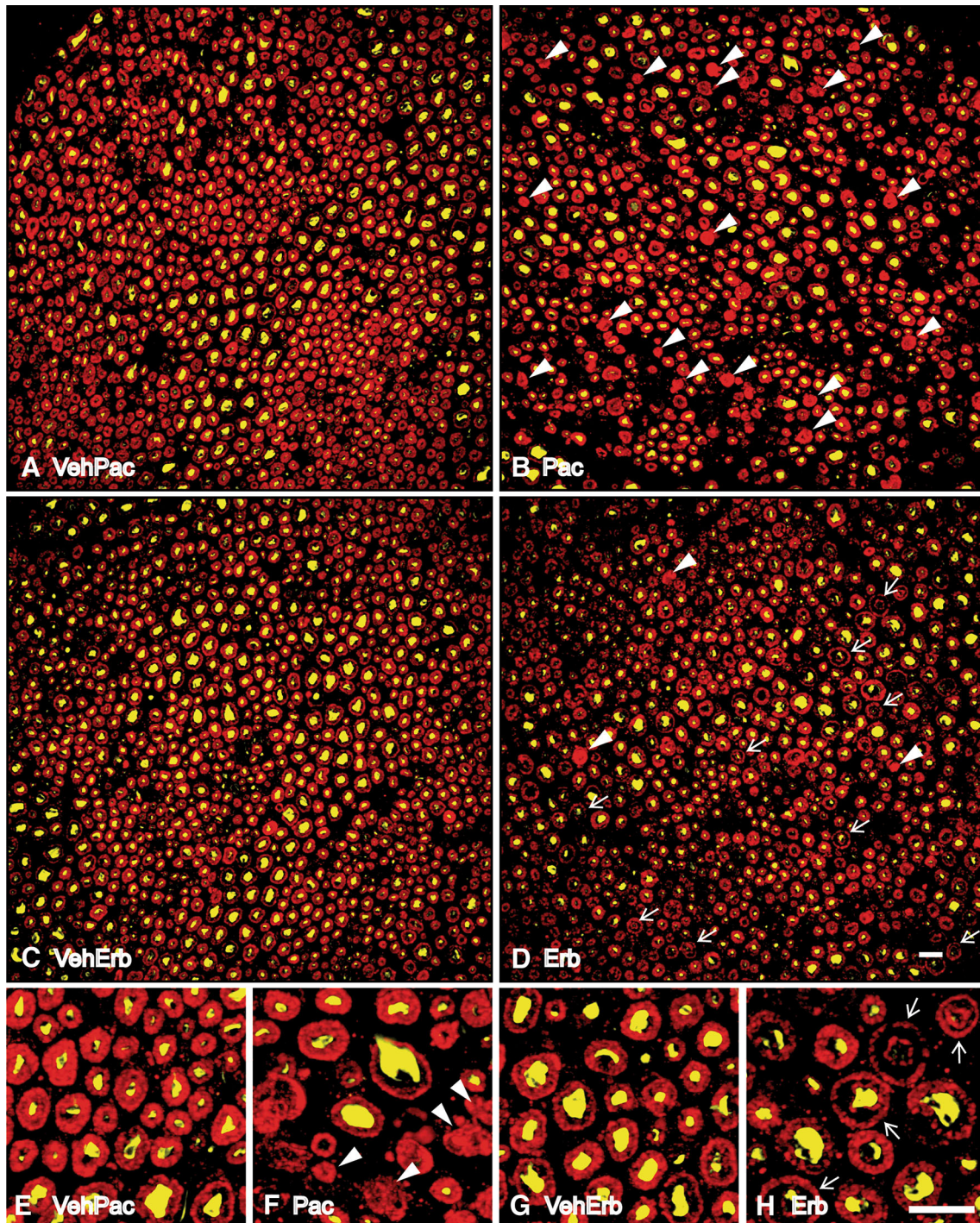
Fig. 2 Paclitaxel and eribulin differentially disrupt normal myelin morphology and differentially lead to degradation of myelin sheaths. **a**, **b** Phosphoneurofilament (PNF; *yellow*) and myelin basic protein (MBP; *red*) expression in sciatic nerve tissue from mice treated with the vehicle for paclitaxel and paclitaxel. Tissue from mice treated with paclitaxel shows frequent signs of axon degeneration (*white arrowheads*) and increased fragmentation. **c**, **d** PNF and MBP expression in vehicle for eribulin and eribulin-treated nerves. Tissue from mice treated with eribulin reveals fewer signs of axon degeneration but occasional instances of thinly myelinated axon fibers and separation of myelin layers ("halos"; *white arrows*) accompanied by myelin fragmentation. **e**, **f** Enlarged views of vehicle paclitaxel and paclitaxel treatments, respectively. **g**, **h** Enlarged regions of vehicle eribulin and eribulin, respectively. *Scale bars* 10 μm
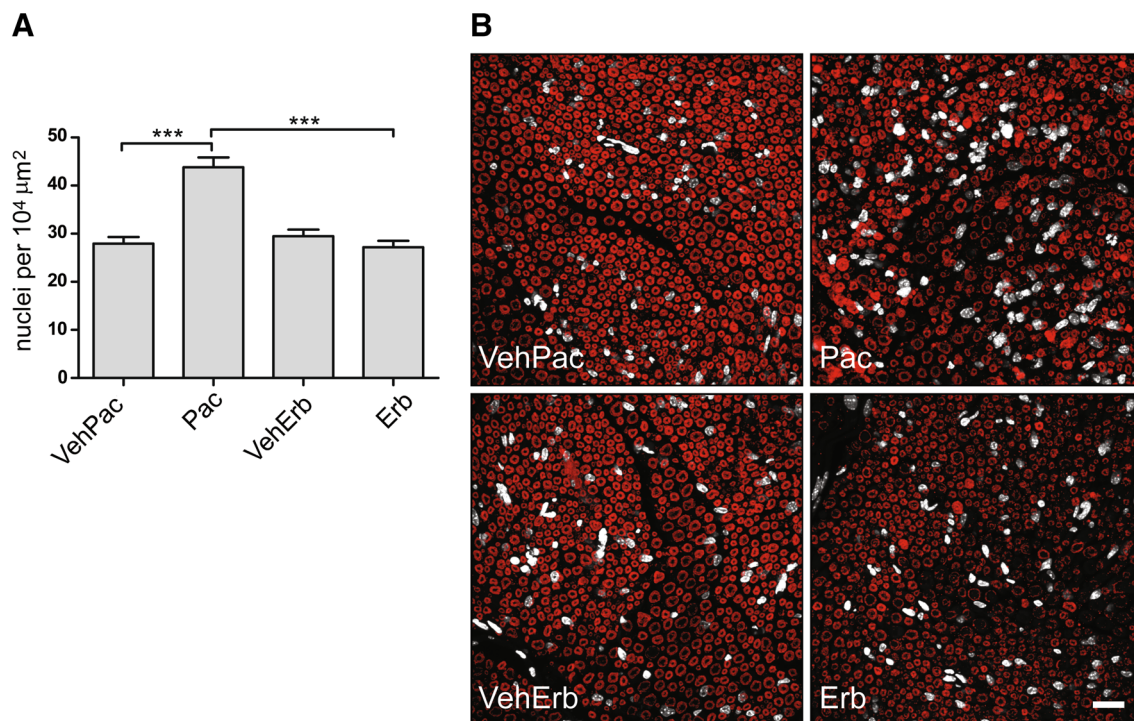
A

B

Fig. 3 Paclitaxel but not eribulin treatment leads to increased numbers of non-neuronal nuclei. **a** Quantification of non-neuronal nuclei present in drug and control nerves ($n = 5$, ***$p < 0.0003$)

b Representative images showing DAPI stained nuclei (*white*) and myelin basic protein (*red*) for reference; *scale bar* 20 µm

Finally, we occasionally observed an unusual morphology, specifically, a thinly myelinated axon fiber within a separated and larger diameter concentric myelin ring, which we have termed a "halo" or "double ring". [Figure 2d, h (see arrows)]. This feature was more commonly observed in eribulin than paclitaxel-treated nerves, and very infrequent in vehicle treatments.

We next hypothesized that there could be changes among the non-neuronal cell population within the nerve in response to neurodegenerative processes. As the cell nuclei for sciatic nerve axons are located within the dorsal root ganglia far from the site of our sectioning, any nuclei present in our images must be non-neuronal. We quantified the population of nuclei present in the sections by staining with DAPI (Fig. 3a, b). Paclitaxel treatment significantly increased the average number of non-neuronal nuclei present from $28.0 \pm$ SEM 1.4 per 10^4 µm² in the vehicle control to $43.8 \pm$ SEM 2.0 per 10^4 µm² in the paclitaxel-treated nerves ($p < 0.0003$). In contrast, there was no significant difference in the average number of nuclei present in eribulin-treated nerves ($29.48 \pm$ SEM 1.4 per 10^4 µm²) versus vehicle-treated nerves ($27.2 \pm$ 1.3; per 10^4 µm²).

In summary, paclitaxel more potently induced deleterious morphological effects, correlating with its greater probability of inducing severe CIPN relative to eribulin.

Paclitaxel and Eribulin Differentially Affect Tubulin Composition

Axons of long peripheral neurons are highly sensitive to changes to the normal balances between microtubule stability, dynamic instability and changes in tubulin post-translational modifications (Almeida-Souza et al. 2011; Avila et al. 1994; Matsuyama and Jarvik 1989). Given that paclitaxel and eribulin each possess different mechanistic capabilities targeted at microtubules, we hypothesized that sciatic nerves from drug-treated mice might exhibit drug-specific effects upon their microtubule biochemistry. We stained nerves from drug-treated and vehicle-treated mice with antibodies specific to α-tubulin and acetylated tubulin. Axons from eribulin-treated sciatic nerves exhibited a marked, statistically significant 2.6-fold increase in α-tubulin signal, from $12.6 \pm$ SEM 3.0 fluorescence units for controls to $32.5 \pm$ SEM 3.7 fluorescence units for eribulin treatment ($p < 0.0167$; Fig. 4a, b). Axons from paclitaxel-treated mice trended toward a smaller increase in α-tubulin signal relative to vehicle-treated mice (1.9-fold; $16.4 \pm$ SEM 2.7 and $8.5 \pm$ SEM 1.1, respectively ($p = 0.0246$ ($p > 0.167$), and $p < 0.0167$ when paclitaxel and eribulin groups are compared, Fig. 4a, b). While not statistically significant when the multiple comparison penalty is applied with a minimum significance threshold
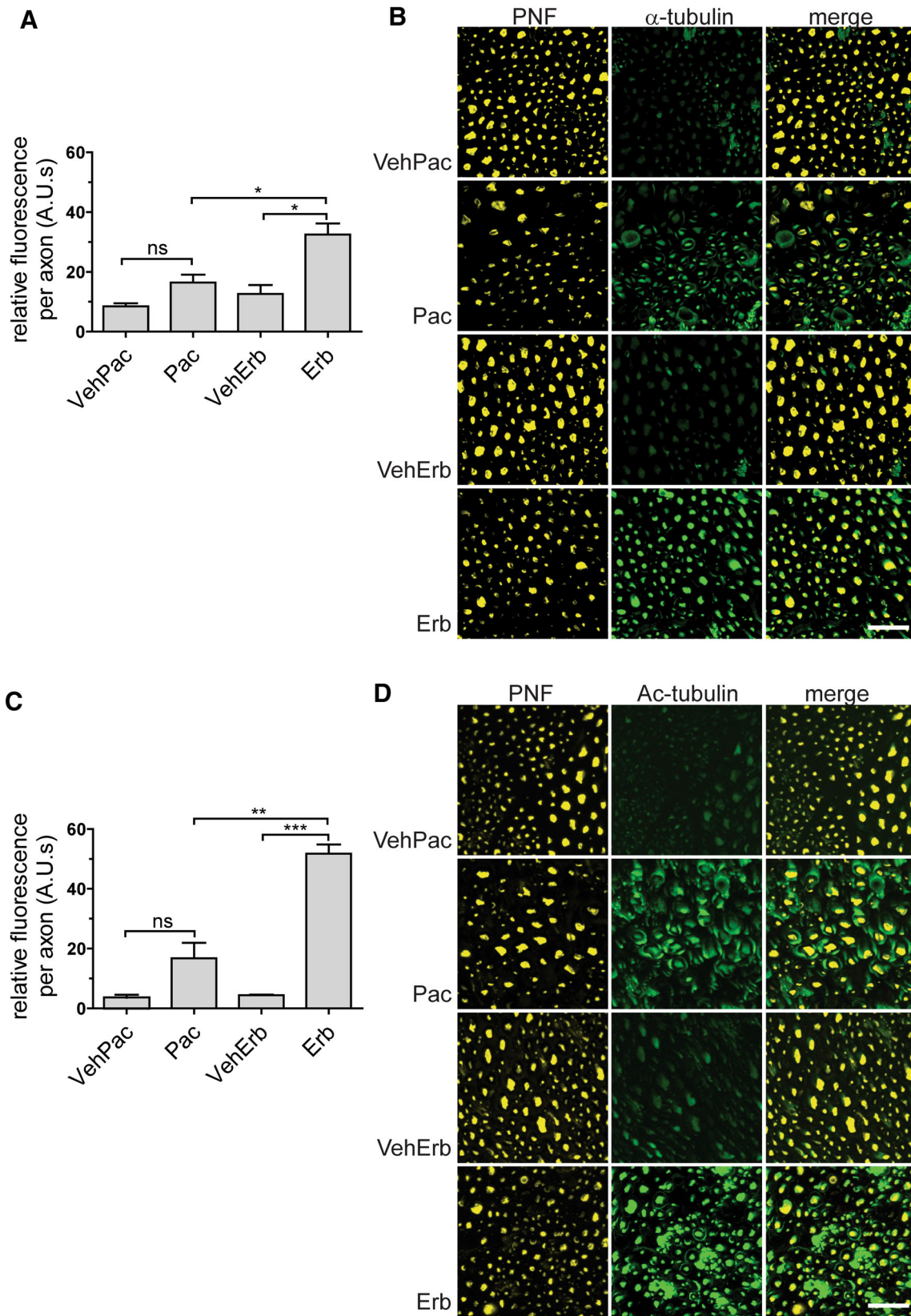
◀**Fig. 4** Eribulin induces greater α-tubulin abundance and tubulin acetylation than paclitaxel. **a** Quantification of tubulin levels in drug and vehicle-treated nerves. Eribulin increased axonal levels of tubulin ∼2.6-fold relative to control ($n = 5$, *$p < 0.0167$) while paclitaxel increased axonal tubulin ∼1.9-fold ($n = 5$, $p = 0.0246$ ($p > 0.0167$))(Paclitaxel compared to eribulin, *$p < 0.0167$). **b** Representative images immunostained for α-tubulin (*green*) and quantified within the axon region defined by PNF signal (*yellow*). Acquisition settings were adjusted to the brightest-fluorescing tissue section. Therefore, because of the pronounced difference in relative fluorescence, the less intensely fluorescing sections appear quite dim. Please see materials and methods for more detail. **c** Quantification of acetylated tubulin levels in drug and control nerves. Paclitaxel treatment increased axonal acetylated tubulin ∼4.6-fold relative to control ($n = 5$, $p = 0.0349$ ($p > 0.0167$)) while eribulin increased axonal acetylated tubulin ∼11.7-fold compared to its control ($n = 5$, ***$p < 0.0003$, paclitaxel compared to eribulin: **$p < 0.003$). **d** Representative images of sciatic nerve tissue, acetylated tubulin (*green*) was quantitated within the axon region defined by PNF. *Scale bars* 20 μm

0.0167, the p value is significant when a standard Student's t test ($p < 0.05$) is applied to singularly test the difference between the means of paclitaxel and its vehicle. Increased tubulin levels have been observed as a result of paclitaxel treatment in multiple cell types (Banerjee 2002; Ranganathan et al. 1998), therefore, we believe that this increase is worthy of consideration. These inductions are especially remarkable considering the high abundance of tubulin in neurons under normal conditions, especially in axons. To control for the artifactual possibility that these increased signals resulted from a constant signal being concentrated into a smaller area because of axon diameter constriction, we quantified the axon surface area and average axon diameters for paclitaxel-treated, eribulin-treated, and vehicle-treated nerves. No changes in either parameter or G-ratio (outer diameter of the myelin sheath to the diameter of the axonal PNF signal, supplemental figure S2) were observed. Additionally, α-tubulin fluorescence intensity did not correlate positively with axon size (Figure S3).

We next assessed changes in tubulin acetylation, a post-translational marker of stable microtubules. Not surprisingly given its mechanism of action, paclitaxel increased axonal acetylated tubulin expression relative to vehicle controls by 4.6-fold (16.8 ± SEM 5.1 and 3.6 ± SEM 1.0, respectively; $p = 0.0349$; Fig. 4c, d). These data demonstrate a clear trend supported by the well-established notion that paclitaxel increases microtubule acetylation in treated cells (de Pennart et al. 1988; Piperno et al. 1987). On the other hand, given that eribulin can promote microtubule depolymerization in vitro and upon short-term administration to cultured cells, it was surprising to observe that eribulin treatment dramatically increased axonal acetylated tubulin expression relative to vehicle controls by 11.7-fold (51.8 ± SEM 3.01 and 4.4 ± SEM 0.24, respectively;

$p < 0.0003$; Fig. 4c, d), demonstrating a remarkably greater increase in tubulin acetylation compared to paclitaxel ($p < 0.0003$). Similarly to α-tubulin, this effect was not dependent upon axon size (Supplemental Figure S3).

These quantitative analyses allow us to calculate the effect of these two drugs upon the ratio of acetylated tubulin to total tubulin relative to their vehicle controls; this ratio should be a measure of drug-induced microtubule stability (Tables 1, 2). Eribulin treatment increases the acetylated tubulin to total tubulin ratio by 4.5-fold relative to its vehicle control whereas paclitaxel treatment increases this ratio by only 2.4-fold relative to its vehicle control.

Eribulin but not Paclitaxel Treatment Increases the Abundance of EB1; Neither Drug Affects EB3 Levels

The microtubule End Binding proteins 1 and 3 (EB1 and EB3) are two highly conserved microtubule binding proteins that selectively track with the plus ends of growing microtubules (Akhmanova and Steinmetz 2008; Jiang and Akhmanova 2011; Jimenez-Mateos et al. 2005; Moughamian et al. 2013). As a result, increased quantities of EB1and/or EB3 are indicative of an increase in the number of growing microtubule ends. Treatment with eribulin induced a ∼2.2-fold increase of immunofluorescence signal for EB1 ($p < 0.0003$) relative to vehicle controls (26.8 ± SEM 0.9 vs. 12.0 ± SEM 0.7, respectively; Fig. 5a, b) and was significantly different compared to the tissue from paclitaxel-treated mice ($p < 0.0003$). This effect is apparent in axons with a wide range of diameters, as demonstrated in heat maps of tissue sections showing the relative intensity of EB1-associated fluorescence (Figure S3). In contrast, paclitaxel did not cause a significant change in the quantity of axonal EB1compared to controls (12.2 ± SEM 1.4 and 10.7 ± SEM 0.57, respectively; Fig. 5a). Finally, no statistically significant changes to

Table 1 Fold Change in abundance following drug treatment (drug/vehicle)

	Erb	Pac
α-tubulin	2.6	1.9
Ac-Tubulin	11.7	4.6
EB1	2.2	1.1

Table 2 Ratios of fold change in abundance following drug treatments

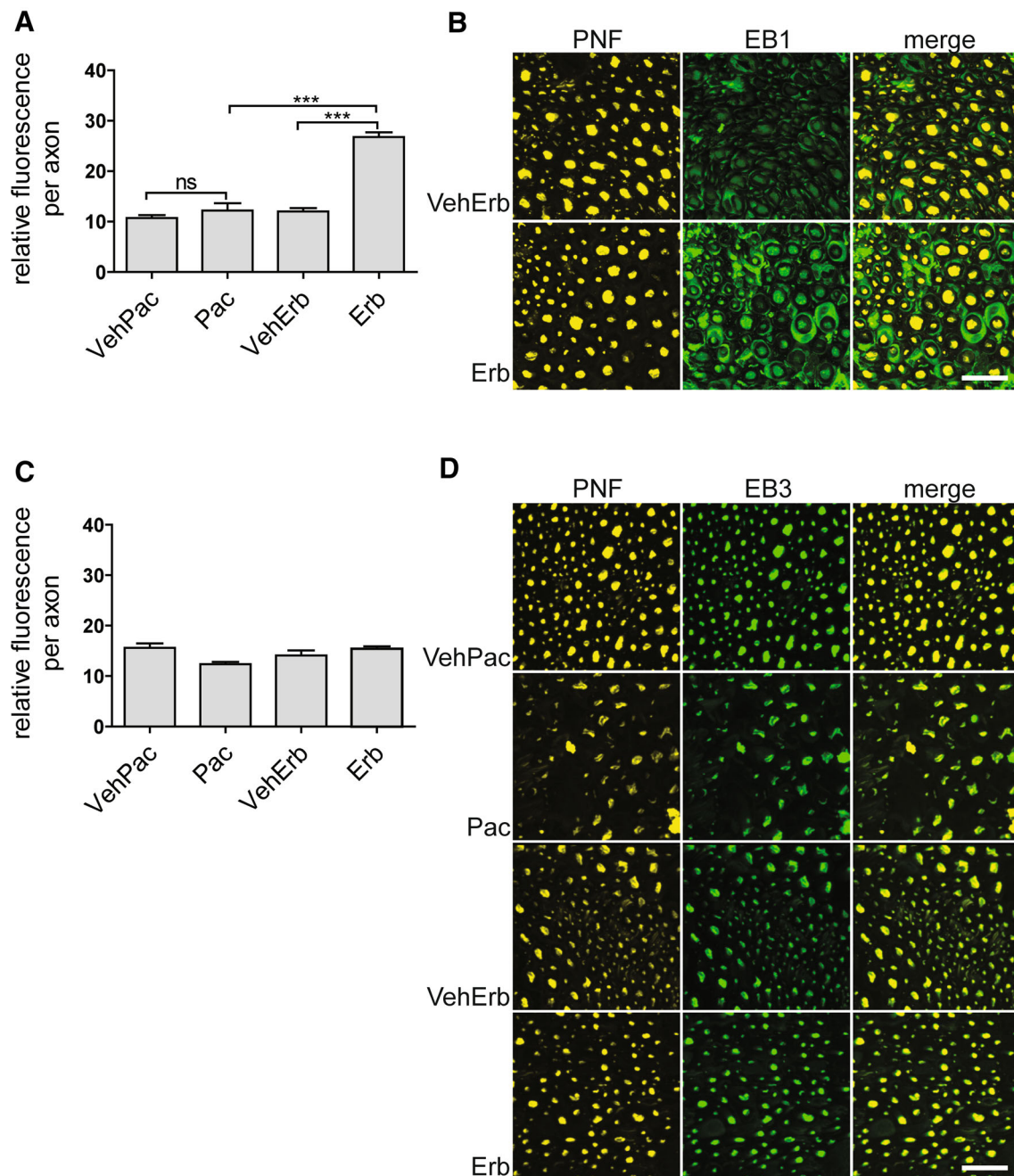|	Erb	Pac
Ac-tub/α-tub	4.5	2.4
EB1/α-tub	0.85	0.58

Fig. 5 Eribulin but not Paclitaxel induces EB1 abundance in axons and Schwann cells; Paclitaxel but not Eribulin reduces EB3 abundance in axons and Schwann cells. **a** Quantification of EB1 levels in drug and control nerves. Axonal EB1 in eribulin-treated nerves increased $\sim$2.2-fold as compared to controls ($n = 5$, ***$p < 0.0003$). No change is observed following paclitaxel treatment as compared to its vehicle. **b** Representative nerve section images; axons are identified by phosphoneurofilament (PNF, *yellow*), EB1 (*green*). Qualitatively, an increase in EB1 abundance was observed in surrounding Schwann cells. **c** EB3 levels did not significantly change with either paclitaxel or eribulin treatment. **d** Representative nerve section images; axons are identified by anti-phosphoneurofilament (PNF, *yellow*, *left panel*), EB3 (*green*, *middle panel*), merge seen in *right panel*. Scale bars 20 μm

axonal EB3 levels were observed with either paclitaxel or eribulin treatment (Fig. 5c, d).

Using the same rationale as used above for acetylated and total tubulin, we calculated the ratio of EB1 and EB3 to total tubulin for each drug treatment relative to its control.

These ratios should be indicators of drug-induced microtubule growing events (Tables 1, 2). The EB1 to tubulin ratio is higher following eribulin treatment than following paclitaxel treatment, suggesting greater microtubule growth in long-term eribulin-treated nerves compared with

long-term paclitaxel-treated nerves. The EB3 to tubulin ratio is the same following eribulin and paclitaxel treatment.

Discussion

In order to begin to identify and dissect molecular mechanisms underlying the initiation and progression of anti-cancer chemotherapy-induced peripheral neuropathy, we compared drug-induced changes in sciatic nerve tissue between mice treated with one of two microtubule targeting chemotherapeutic agents—paclitaxel, a drug commonly used in the clinic that causes relatively high frequencies of severe peripheral neuropathy and eribulin, a less commonly used drug that induces a lower frequency of severe neuropathic side effects. We sought to ask how these two different microtubule targeting drugs affect mouse sciatic nerve morphology and biochemistry. From our observations of both motor and sensory neurons (both of which may be affected in severe neuropathy), we seek to pose testable hypotheses focusing upon the induction and progression of peripheral neuropathy.

Our most important results are

1. Both paclitaxel and eribulin trended toward axon loss;
2. Systemic administration of paclitaxel, and to a lesser extent eribulin increased signs of axon degeneration.
3. Systemic administration of paclitaxel, but not eribulin,

   a. Increased the abundance of non-neuronal cells.

4. Systemic administration of eribulin, and to a lesser extent paclitaxel.

   a. Induced total tubulin accumulation;
   b. Induced tubulin acetylation, a marker for microtubule stability.

5. Systemic administration of eribulin, but not paclitaxel.

   a. Increased the abundance of myelin halos/double rings.
   b. Increased the abundance of EB1, a marker for growing microtubules.

These observations demonstrate that paclitaxel and eribulin each exert quantitatively and qualitatively distinct effects on axon degeneration, myelin morphology, and microtubule composition in mouse sciatic nerve tissue. Further, the data indicate that paclitaxel treatment is much more potent than eribulin with respect to inducing signs of axon degeneration, while eribulin more effectively induces potentially positive biochemical effects (i.e., increased levels of tubulin, tubulin acetylation, and EB1).

Based on these observations, we propose that the greater clinical probability of severe peripheral neuropathy by paclitaxel relative to eribulin may be a function of its greater relative damage to the nervous system coupled with eribulin's ability to promote a more stable and growth oriented microtubule network than does paclitaxel. With respect to the latter, we note that the regulation of microtubule dynamics is a balancing act between microtubule shortening events, microtubule lengthening events and a population of stable non-changing microtubules. We propose that the long-term combined effects of increased total tubulin (providing more building blocks for microtubule assembly), tubulin acetylation (indicating greater microtubule stability), and EB1 (suggesting more growing microtubule ends) more than compensate for eribulin's inherent ability to suppress microtubule growth events (see below for more discussion). The net effect is an extensive and functional microtubule network. Such a compensatory or neuroprotective mechanism could also be at play in electrophysiological experiments demonstrating that paclitaxel but not eribulin causes a loss of caudal nerve amplitude and reduced conduction velocity (Wozniak et al. 2011); indeed, eribulin administration actually increases caudal nerve amplitude and exhibits no reduction in conduction velocity in these studies. Wozniak et al. (2011) also observed signs of axon degeneration, similar to those described in this work, more frequently in tissue from paclitaxel-treated mice as compared to eribulin-treated mice, correlating with the functional deficits seen in paclitaxel, but not eribulin. Unfortunately, due to the higher level of drug required to achieve a MTD, we are unable perform functional assessments on the same mice receiving drugs. However, based upon previous data, we predict that paclitaxel would demonstrate greater functional deficits compared to eribulin, but lack the ability to make direct conclusions at this time.

Morphological Considerations

Most prominently, we observed both paclitaxel and eribulin disrupted normal myelin morphology in a fraction of the neurons. Quantitatively, these indications of axon degeneration were more frequently observed in tissue after paclitaxel treatment compared to tissue after eribulin treatment ($p < 0.003$), suggesting that paclitaxel was more potent in causing neurodegeneration. On the other hand, although losses in axon density were observed after treatment with either drug, these losses did not reach statistical significance at our statistical thresholds. Three reasons that may account for the lack of statistical significance (and only trends) in observed axon losses are (i) that our sampling region within the mid-thigh region is a relatively

great distance from the distal nerve endings where morphological consequences are most pronounced (Boyette-Davis et al. 2011), (ii) there may be a high degree of individual variability in the number of neurons that retract over that distance, and (iii) there may enough mouse to mouse variability in axon density so as to obscure subtle differential drug-induced effects. Given these considerations, we believe that disruption of the normal myelin expression pattern is a better measure of drug-induced degenerative effects than is axon loss.

At the same time, we note that eribulin does induce more myelin halos than does paclitaxel. We speculate that these may represent a relatively early stage of the neurodegenerative process. These observations are consistent with recent work by Vahdat et al., and colleagues who found that the onset of eribulin-induced neuropathy occurred later than that induced by the microtubule stabilizing drug ixabepilone, which normally displays a higher incidence of neuropathy than paclitaxel (Steinberg 2008; Vahdat et al. 2013).

Mechanistic Considerations

Perhaps the most surprising observations presented here are that long-term eribulin treatment leads to a marked increase in the abundance of both total tubulin and acetylated tubulin. The simplest interpretation of these observations is that eribulin treatment results in an increase in the abundance of stable microtubules. This is surprising because eribulin is generally viewed as a microtubule depolymerizing agent. However, it is important to emphasize that the previously demonstrated microtubule depolymerizing activity of eribulin has been observed in short-term in vitro biochemical reactions or when added to proliferating cultured cells for a few hours. In contrast, our investigations were performed following 2 weeks of systemic drug administration to mice and focused primarily on post-mitotic neurons. Mechanistically, one could imagine that microtubules in the sciatic nerve might exhibit net depolymerization upon initial exposure to eribulin. However, either depolymerization itself or some other aspect of eribulin action leads to subsequent regulatory mechanisms that induce tubulin levels, tubulin acetylation levels, EB1 levels and perhaps additional proteins. As one possibility, the binding of eribulin to free tubulin subunits may inactivate the normal tubulin auto-regulatory mechanism by which free tubulin subunits bind to tubulin mRNA and thereby promote tubulin mRNA degradation, which in turn leads to a reduction of tubulin protein synthesis (Gay et al. 1987; Pachter et al. 1987). By this mechanism, eribulin would inhibit tubulin mRNA turnover, leading to the accumulation of increased levels of tubulin mRNA and tubulin protein. Together, these stabilizing effects could compensate for the destabilizing effects of eribulin on the microtubule network, leading to a more robust and stable microtubule network that can function relatively effectively. These effects may be neuronal specific, thereby providing protection from the drug for neurons while not compromising the action of the drug on tumor cells.

Another possibility that must be considered is that perhaps eribulin does not effectively get into the nerve and this underlies its reduced frequency of severe CIPN. We think this is extremely unlikely. Indeed, recent work from some of our labs directly assessed the pharmacokinetics and peripheral nerve distribution of eribulin and paclitaxel following administration via the caudal vein (unpublished data, KW, BAL, BSS). Both drugs rapidly penetrated the sciatic nerves and dorsal root ganglia, with maximal concentrations achieved within 15 min. With the passage of time, dose normalized area under the curve in the sciatic nerves was actually greater for eribulin than for paclitaxel. These findings indicate that limited peripheral nerve exposure is likely not the underlying mechanism for the differential propensity of eribulin and paclitaxel to produce neurotoxicity.

The increase in total tubulin in both eribulin and paclitaxel-treated cells provides an enormous supply of additional microtubule building blocks. Given sufficient GTP and growth and/or stabilization regulatory cues, this would enable the neuronal cells to markedly augment their microtubule networks. The increased ratios of acetylated tubulin to total tubulin in drug versus vehicle axons suggest drug-induced microtubule stability. The fact that this ratio is 1.9-fold greater in eribulin-treated nerves than in paclitaxel-treated nerves (4.5/2.4; Tables 1, 2) implies that the microtubule network in eribulin-treated nerves is considerably more stable than in paclitaxel-treated nerves. It is also interesting to consider recent work demonstrating that tubulin acetylation can also influence the interaction between MAPs and microtubules. For example, recent work suggests that tubulin acetylation may, in part, control the affinity between microtubules and kinesin (Almeida-Souza et al. 2011; Dompierre et al. 2007; Reed et al. 2006; Walter et al. 2012).

Increased levels of EB1 may also play an important role in eribulin's relatively benign induction of CIPN via a number of possible mechanisms. Similarly to acetylation, the EB1 to total tubulin ratio in drug-treated versus control axons is higher for eribulin than for paclitaxel treatment. This higher ratio of EB1 to total tubulin suggests a greater proportion of growing microtubule plus ends in eribulin versus paclitaxel treatment. Additionally, evidence suggests that EB1 can promote de-novo microtubule nucleation (Vitre et al. 2008). Finally, EB1 is known to influence microtubule dynamics both directly and indirectly. Upon binding directly to microtubule plus ends EB1 recognizes GTP tubulin and an intermediate form as tubulin changes

from GTP to GDP bound, preferentially binding the intermediate form and increasing the rate of tubulin maturation to stable, polymerized GDP-bound tubulin (Kumar and Wittmann 2012; Maurer et al. 2012). This action directly influences microtubule dynamicity. EB1 can also influence microtubule dynamics indirectly via its recruitment of other proteins known to influence microtubule dynamics, including +TIPS such as the CLIP family members, CLASPs and APC as well as XMAP (Akhmanova and Steinmetz 2008).

Increased Population of Non-neuronal Cells in Paclitaxel-Treated Nerves

Our data demonstrate that paclitaxel but not eribulin treatment increases the number of non-neuronal nuclei (and hence cells) present in sciatic nerve tissue. Schwann cells likely account for the majority of nuclei found in tissue from vehicle and eribulin-treated mice. However, the identity of the additional cells seen in paclitaxel-treated nerves is less obvious. Increased Schwann cell division could account for the increased nuclear population, but invasion by immune cells responding to degenerative axons may also contribute to the effect. Invasion of the sciatic nerve by immune cells and release of pro-inflammatory factors have been observed after nerve injury and neuropathic pain-inducing paclitaxel treatment (Janes et al. 2014; Peters et al. 2007a, b; Rotshenker 2011).

Eribulin and Paclitaxel: Anti-Cancer Efficacy

The demonstration that eribulin induces less frequent severe CIPN than the widely used paclitaxel raises the question of its relative anti-cancer efficacy relative to paclitaxel. A lower incidence of severe peripheral neuropathy would be most meaningful if it were coupled with equal or greater anti-cancer efficacy. Unfortunately, to date there have been no completed clinical studies directly comparing the anti-cancer efficacies of eribulin and paclitaxel in the clinical setting. That said, eribulin was FDA approved in 2010 as a third line therapy for patients with metastatic breast cancer who had previously received at least two prior chemotherapy regimens, including an anthracycline and a taxane. At the time of the pivotal Phase III EMBRACE trial which led to the FDA approval, there was no standard of care for third line metastatic breast cancer, so EMBRACE was designed, in conjunction with the FDA, as a two-arm study of eribulin monotherapy versus "treatment of physician's choice" (TPC), essentially capturing the individual judgements of hundreds of oncologists' decisions as to the best personalized treatment of those specific patients (Cortes et al. 2012). EMBRACE stipulated that enrolled patients must have progressed within 6 months or less of the latest chemotherapy (Cortes et al. 2012). As such, the statistically significant 24 % increase in median overall survival between the two groups (13.1 months vs. 10.6 months for eribulin versus TPC, respectively) indicates that many patients enjoyed prolonged survival on the eribulin arm despite the fact that they had previously progressed on taxane-containing therapies. In addition, the preclinical work of Towle et al. (2001), demonstrated that eribulin is more effective at considerably lower doses than paclitaxel (at empirically determined MTD levels) in four different human tumor xenograft growth models in mice: potency differentials for eribulin versus paclitaxel based on complete tumor suppression ranged from 20- to 100-fold for different human tumors. Additionally, in these in vivo studies, eribulin consistently showed a wider therapeutic window compared to paclitaxel. Finally, eribulin showed an average 4.1-fold increased potency compared to paclitaxel on a molar basis in a library of eight human cancer cell lines, with ratios in the individual lines ranging from 2.0-fold to 27.8-fold. We conclude that, although direct head-to-head comparisons of eribulin versus paclitaxel have yet to be reported in the clinical setting, existing clinical evidence from the EMBRACE Phase III clinical trial pointing to eribulin activity after progression on taxanes, coupled with consistent preclinical evidence of greater potency both in cancer cell lines and human tumor xenograft models, make a compelling case that eribulin is either an equipotent or more potent anti-cancer agent relative to paclitaxel. In this context, the apparently lower neuropathic effects of eribulin relative to paclitaxel in both the clinic and laboratory settings can be viewed as not simply a consequence of lower overall potency, but rather a bona fide reduction in one of the most significant and troubling side effects of treatment with these two agents.

Summary

Work presented here leads us to hypothesize that long-term treatment with eribulin generates a more functional microtubule cytoskeleton than does similar treatment with paclitaxel, accounting at least in part for the reduced levels of severe CIPN observed with eribulin-treated versus paclitaxel-treated patients. With this foundation, future investigations will include testing this hypothesis mechanistically, both in animal and cell culture models.

References

Akhmanova A, Steinmetz MO (2008) Tracking the ends: a dynamic protein network controls the fate of microtubule tips. Nat Rev Mol Cell Biol 9:309–322. doi:10.1038/nrm2369

Almeida-Souza L, Timmerman V, Janssens S (2011) Microtubule dynamics in the peripheral nervous system: A matter of balance. Bioarchitecture 1:267–270. doi:10.4161/bioa.1.6.19198

Argyriou AA, Marmiroli P, Cavaletti G, Kalofonos HP (2011) Epothilone-induced peripheral neuropathy: a review of current knowledge. J Pain Symptom Manage 42:931–940. doi:10.1016/j.jpainsymman.2011.02.022

Argyriou AA, Bruna J, Marmiroli P, Cavaletti G (2012) Chemotherapy-induced peripheral neurotoxicity (CIPN): an update. Crit Rev Oncol Hematol 82:51–77. doi:10.1016/j.critrevonc.2011.04.012

Avila J, Dominguez J, Diaz-Nido J (1994) Regulation of microtubule dynamics by microtubule-associated protein expression and phosphorylation during neuronal development. Int J Dev Biol 38:13–25

Banerjee A (2002) Increased levels of tyrosinated α-, βIII-, and βIV-tubulin isotypes in paclitaxel-resistant MCF-7 breast cancer cells. Biochem Biophys Res Commun 293:598–601. doi:10.1016/S0006-291X(02)00269-3

Boehmerle W, Huehnchen P, Peruzzaro S, Balkaya M, Endres M (2014) Electrophysiological, behavioral and histological characterization of paclitaxel, cisplatin, vincristine and bortezomib-induced neuropathy in C57Bl/6 mice. Sci Rep 4:6370. doi:10.1038/srep06370

Boyette-Davis J, Xin W, Zhang H, Dougherty PM (2011) Intraepidermal nerve fiber loss corresponds to the development of taxol-induced hyperalgesia and can be prevented by treatment with minocycline. Pain 152:308–313. doi:10.1016/j.pain.2010.10.030

Bunker JM, Wilson L, Jordan MA, Feinstein SC (2004) Modulation of microtubule dynamics by tau in living cells: implications for development and neurodegeneration. Mol Biol Cell 15:2720–2728. doi:10.1091/mbc.E04-01-0062

Carlson K, Ocean AJ (2011) Peripheral neuropathy with microtubule-targeting agents: occurrence and management approach. Clin Breast Cancer 11:73–81. doi:10.1016/j.clbc.2011.03.006

Choi YJ, Di Nardo A, Kramvis I, Meikle L, Kwiatkowski DJ, Sahin M, He X (2008) Tuberous sclerosis complex proteins control axon formation. Genes Dev 22:2485–2495

Cortes J, Montero AJ, Gluck S (2012) Eribulin mesylate, a novel microtubule inhibitor in the treatment of breast cancer. Cancer Treat Rev 38:143–151. doi:10.1016/j.ctrv.2011.03.006

Creppe C, Malinouskaya L, Volvert ML, Gillard M, Close P, Malaise O, Laguesse S, Cornez I, Rahmouni S, Ormenese S, Belachew S, Maigrange B, Chapelle JP, Siebenlist U, Moonen G, Chariot A, Nguyen L (2009) Elongator controls the migration and differentiation of cortical neurons through acetylation of alpha-tubulin. Cell 136:551–564. doi:10.1016/j.cell.2008.11.043

de Pennart H, Houliston E, Maro B (1988) Post-translational modifications of tubulin and the dynamics of microtubules in mouse oocytes and zygotes. Biol Cell 64:375–378

Derry WB, Wilson L, Jordan MA (1995) Substoichiometric binding of taxol suppresses microtubule dynamics. Biochemistry 34:2203–2211

Dompierre JP, Godin JD, Charrin BC, Cordelieres FP, King SJ, Humbert S, Saudou F (2007) Histone deacetylase 6 inhibition compensates for the transport deficit in Huntington's disease by increasing tubulin acetylation. J Neurosci 27:3571–3583. doi:10.1523/jneurosci.0037-07.2007

Field JJ, Kanakkanthara A, Miller JH (2014) Microtubule-targeting agents are clinically successful due to both mitotic and interphase impairment of microtubule function. Bioorg Med Chem 22:5050–5059. doi:10.1016/j.bmc.2014.02.035

Gay DA, Yen TJ, Lau JT, Cleveland DW (1987) Sequences that confer beta-tubulin autoregulation through modulated mRNA stability reside within exon 1 of a beta-tubulin mRNA. Cell 50:671–679

Geraldo S, Khanzada UK, Parsons M, Chilton JK, Gordon-Weeks PR (2008) Targeting of the F-actin-binding protein drebrin by the microtubule plus-tip protein EB3 is required for neuritogenesis. Nat Cell Biol 10:1181–1189. doi:10.1038/ncb1778

Godena VK, Brookes-Hocking N, Moller A, Shaw G, Oswald M, Sancho RM, Miller CC, Whitworth AJ, De Vos KJ (2014) Increasing microtubule acetylation rescues axonal transport and locomotor deficits caused by LRRK2 Roc-COR domain mutations. Nat Commun 5:5245. doi:10.1038/ncomms6245

Gradishar WJ (2011) The place for eribulin in the treatment of metastatic breast cancer. Curr Oncol Rep 13:11–16. doi:10.1007/s11912-010-0145-9

Gu C, Zhou W, Puthenveedu MA, Xu M, Jan YN, Jan LY (2006) The microtubule plus-end tracking protein EB1 is required for Kv1 voltage-gated K+ channel axonal targeting. Neuron 52:803–816. doi:10.1016/j.neuron.2006.10.022

Heller BA, Ghidinelli M, Voelkl J, Einheber S, Smith R, Grund E, Morahan G, Chandler D, Kalaydjieva L, Giancotti F, King RH, Fejes-Toth AN, Fejes-Toth G, Feltri ML, Lang F, Salzer JL (2014) Functionally distinct PI 3-kinase pathways regulate myelination in the peripheral nervous system. J Cell Biol 204:1219–1236. doi:10.1083/jcb.201307057

Janes K, Little JW, LI C, CBryant L, Chen C, Chen Z, Kamocki K, Doyle T, Snider A, Esposito E, Cuzzocrea S, Bieberich E, Obeid L, Petrache I, Nicol G, Neumann WL, Salvemini D (2014) The development and maintenance of paclitaxel-induced neuropathic pain require activation of the sphingosine 1-phosphate receptor subtype 1. J Biol Chem 289:21082–21097. doi:10.1074/jbc.M114.569574

Jaworski J, Kapitein LC, Gouveia SM, Dortland BR, Wulf PS, Grigoriev I, Camera P, Spangler SA, Di Stefano P, Demmers J, Krugers H, Defilippi P, Akhmanova A, Hoogenraad CC (2009) Dynamic microtubules regulate dendritic spine morphology and synaptic plasticity. Neuron 61:85–100. doi:10.1016/j.neuron.2008.11.013

Jiang K, Akhmanova A (2011) Microtubule tip-interacting proteins: a view from both ends. Curr Opin Cell Biol 23:94–101. doi:10.1016/j.ceb.2010.08.008

Jimenez-Mateos EM, Paglini G, Gonzalez-Billault C, Caceres A, Avila J (2005) End binding protein-1 (EB1) complements microtubule-associated protein-1B during axonogenesis. J Neurosci Res 80:350–359. doi:10.1002/jnr.20453

Jordan MA, Wilson L (2004) Microtubules as a target for anticancer drugs. Nat Rev Cancer 4:253–265. doi:10.1038/nrc1317

Jordan MA, Kamath K, Manna T, Okouneva T, Miller HP, Davis C, Littlefield BA, Wilson L (2005) The primary antimitotic mechanism of action of the synthetic halichondrin E7389 is suppression of microtubule growth. Mol Cancer Ther 4:1086–1095. doi:10.1158/1535-7163.mct-04-0345

Kumar P, Wittmann T (2012) +TIPs: SxIPping along microtubule ends. Trends Cell Biol 22:418–428. doi:10.1016/j.tcb.2012.05.005

Lapointe NE, Morfini G, Brady ST, Feinstein SC, Wilson L, Jordan M (2013) Effects of eribulin, vincristine, paclitaxel and ixabepilone on fast axonal transport and kinesin-1 driven microtubule gliding: Implications for chemotherapy-induced peripheral neuropathy. Neurotoxicology. doi:10.1016/j.neuro.2013.05.008

Levy DB, Smith KJ, Beazer-Barclay Y, Hamilton SR, Vogelstein B, Kinzler KW (1994) Inactivation of both APC alleles in human and mouse tumors. Cancer Res 54:5953–5958

Matsuyama SS, Jarvik LF (1989) Hypothesis: microtubules, a key to Alzheimer disease. Proc Natl Acad Sci USA 86:8152–8156

Maurer SP, Fourniol FJ, Bohner G, Moores CA, Surrey T (2012) EBs recognize a nucleotide-dependent structural cap at growing microtubule ends. Cell 149:371–382. doi:10.1016/j.cell.2012.02.049

Morfini GA, Burns M, Binder LI, Kanaan NM, LaPointe N, Bosco DA, Brown RH Jr, Brown H, Tiwari A, Hayward L, Edgar J, Nave KA, Garberrn J, Atagi Y, Song Y, Pigino G, Brady ST (2009) Axonal transport defects in neurodegenerative diseases. J Neurosci 29:12776–12786. doi:10.1523/jneurosci.3463-09.2009

Moughamian AJ, Osborn GE, Lazarus JE, Maday S, Holzbaur EL (2013) Ordered recruitment of dynactin to the microtubule plus-end is required for efficient initiation of retrograde axonal transport. J Neurosci 33:13190–13203. doi:10.1523/jneurosci.0935-13.2013

Muguruma T, Sakura S, Kirihara Y, Saito Y (2006) Comparative somatic and visceral antinociception and neurotoxicity of intrathecal bupivacaine, levobupivacaine, and dextrobupivacaine in rats. Anesthesiology 104:1249–1256

Pachter JS, Yen TJ, Cleveland DW (1987) Autoregulation of tubulin expression is achieved through specific degradation of polysomal tubulin mRNAs. Cell 51:283–292

Peters CM, Jimenez-Andrade JM, Jonas BM, Sevcik MA, Koewler JN, Ghilardi JR, Wong GY, Mantyh PW (2007a) Intravenous paclitaxel administration in the rat induces a peripheral sensory neuropathy characterized by macrophage infiltration and injury to sensory neurons and their supporting cells. Exp Neurol 203:42–54. doi:10.1016/j.expneurol.2006.07.022

Peters CM, Jimenez-Andrade JM, Kuskowski MA, Ghilardi JR, Mantyh PW (2007b) An evolving cellular pathology occurs in dorsal root ganglia, peripheral nerve and spinal cord following intravenous administration of paclitaxel in the rat. Brain Res 1168:46–59. doi:10.1016/j.brainres.2007.06.066

Piperno G, LeDizet M, Chang XJ (1987) Microtubules containing acetylated alpha-tubulin in mammalian cells in culture. J Cell Biol 104:289–302

Poruchynsky MS, Komlodi-Pasztor E, Trostel S, Wilkerson J, Regairaz M, Pommier Y, Zhang X, Kumar Maity T, Robey R, Burotto M, Sackett D, Guha U, Fojo AT (2015) Microtubule-targeting agents augment the toxicity of DNA-damaging agents by disrupting intracellular trafficking of DNA repair proteins. Proc Natl Acad Sci USA 112:1571–1576. doi:10.1073/pnas.1416418112

Ranganathan S, Benetatos CA, Colarusso PJ, Dexter DW, Hudes GR (1998) Altered beta-tubulin isotype expression in paclitaxel-resistant human prostate carcinoma cells. Br J Cancer 77:562–566

Reed NA, Cai D, Blasius TL, Jih GT, Meyhofer E, Gaertig J, Verhey KJ (2006) Microtubule acetylation promotes kinesin-1 binding and transport. Curr Biol 16:2166–2172. doi:10.1016/j.cub.2006.09.014

Rotshenker S (2011) Wallerian degeneration: the innate-immune response to traumatic nerve injury. J Neuroinflammation 8:109. doi:10.1186/1742-2094-8-109

Schnaar RL, Gerardy-Schahn R, Hildebrandt H (2014) Sialic acids in the brain: gangliosides and polysialic acid in nervous system development, stability, disease, and regeneration. Physiol Rev 94:461–518. doi:10.1152/physrev.00033.2013

Smith JA, Wilson L, Azarenko O, Zhu X, Lewis BM, Littlefield BA, Jordan MA (2010) Eribulin binds at microtubule ends to a single site on tubulin to suppress dynamic instability. Biochemistry 49:1331–1337. doi:10.1021/bi901810u

Steinberg M (2008) Ixabepilone: a novel microtubule inhibitor for the treatment of locally advanced or metastatic breast cancer. Clin Ther 30:1590–1617. doi:10.1016/j.clinthera.2008.09.015

Towle MJ, Salvato KA, Budrow J, Wels BF, Kuznetsov G, Aalfs KK, Welsh S, Zheng W, Seletsky BM, Palme MH, Habgood GJ, Singer LA, Dipietro LV, Wang Y, Chen JJ, Quincy DA, Davis A, Yoshimatsu K, Kishi Y, Yu MJ, Littlefield BA (2001) In vitro and in vivo anticancer activities of synthetic macrocyclic ketone analogues of halichondrin B. Cancer Res 61:1013–1021

Vahdat LT, Garcia AA, Vogel C, Pellegrino C, Lindquist DL, Iannotti N, Gopalakrishna P, Sparano JsA (2013) Eribulin mesylate versus ixabepilone in patients with metastatic breast cancer: a randomized Phase II study comparing the incidence of peripheral neuropathy. Breast Cancer Res Treat 140:341–351. doi:10.1007/s10549-013-2574-2

Vitre B, Coquelle FM, Heichette C, Garnier C, Chretien D, Arnal I (2008) EB1 regulates microtubule dynamics and tubulin sheet closure in vitro. Nat Cell Biol 10:415–421. doi:10.1038/ncb1703

Walter WJ, Beranek V, Fischermeier E, Diez S (2012) Tubulin acetylation alone does not affect kinesin-1 velocity and run length in vitro. PLoS One 7:e42218. doi:10.1371/journal.pone.0042218

Windebank AJ, Grisold W (2008) Chemotherapy-induced neuropathy. J Peripher Nerv Syst 13:27–46. doi:10.1111/j.1529-8027.2008.00156.x

Wozniak KM, Nomoto K, Lapidus RG, Uw Y, Carozzi V, Cavaletti G, Hayakawa K, Hosokawa S, Towle MJ, Littlefield BA, Slusher BS (2011) Comparison of neuropathy-inducing effects of eribulin mesylate, paclitaxel, and ixabepilone in mice. Cancer Res 71:3952–3962. doi:10.1158/0008-5472.can-10-4184

Zhang T, Yao S, Wang P, Yin C, Xiao C, Qian M, Liu D, Zheng L, Meng W, Zhu H, Liu J, Xu H, Mo X (2011) ApoA-II directs morphogenetic movements of zebrafish embryo by preventing chromosome fusion during nuclear division in yolk syncytial layer. J Biol Chem 286:9514–9525. doi:10.1074/jbc.M110.134908